Original Article

Fluorescence-enabled evaluation of nasal tract deposition and coverage of pharmaceutical formulations in a silicone nasal cast using an innovative spray device

Davide D'Angelo [a,1], Stefan Kooij [b,1], Frank Verhoeven [c], Fabio Sonvico [a,*], Cees van Rijn [b,*]

[a] Food and Drug Department, University of Parma, Parco Area delle Scienze 27/A, 43124 Parma, Italy
[b] Van der Waals-Zeeman Institute, Institute of Physics, University of Amsterdam, Amsterdam 1098XH, the Netherlands
[c] Medspray, Medspray Technology & Manufacturing B.V, Enschede 7521 PV, the Netherlands

HIGHLIGHTS

- A method was optimized for quantifying silicone nasal cast deposition of liquid formulations, using nasal devices.
- Image analysis was completed by fluorometric analysis to overcome the problem of potential underestimation of the image analysis.
- Droplet velocity was a critical parameter, using a device emitting droplets with low initial velocity (<1 m/s), a uniform coverage of the nasal cast was achieved.

GRAPHICAL ABSTRACT
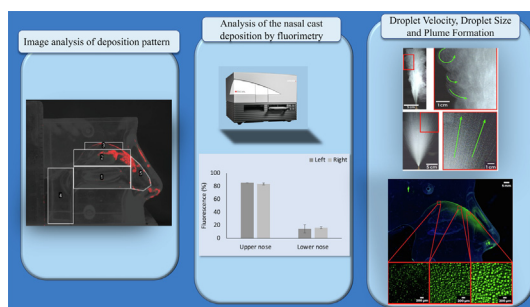
ABSTRACT

Introduction: The characterisation of nasal formulations is a critical point. However, there are still no recommendations or guidelines in terms of standard approaches for evaluating the formulation's nasal deposition and/or coverage profile. This study optimises a method for quantifying silicone nasal cast deposition and coverage of liquid formulations using different nasal devices.
Objectives: The present work investigates the nasal deposition and coverage patterns of innovative nasal spray nozzles producing slow velocity soft mists, using a nasal cavity replica and a fluorescent dye.
Methods: The study of the deposition pattern of a fluorescent liquid formulation in a transparent nasal cast was carried out in both the presence and absence of a simulated inhalation flow. The extent of the deposition pattern was investigated using ImageJ and fluorescence in the nasal cast, quantified by fluorometric analysis. The particle size distribution and initial droplet velocity were determined using a laser diffractometer and a high-speed camera with a frame rate of 1000 fps.
Results: A uniform intranasal coverage was obtained with droplets of a volume median particle size (Dv50) between 15 and 25 μm in airflow between 10 and 30 L/min. In these conditions, aerosol formulations can be uniformly deposited in the vestibule and turbinate cavity nasal regions, with less than 10 % passing beyond the nasopharyngeal region.

Conclusion: The method applied allowed for the determination of the coverage of the nasal cast in different regions using images analysis and fluorometric analysis. Droplet velocity is a critical parameter in the deposition in the nasal cavity. With standard swirl nozzles, many droplets are found on the surface of the nasal vestibule. Soft mist nozzles produce smaller droplets at a much lower initial velocity (<1 m/s), resulting in a more uniform coverage.

Introduction

For many years, nasal administration has been limited to the local delivery of antihistamines and corticosteroids. However, the peculiar characteristics of this anatomical region offer a suitable route for systemic administration of many drugs, including biopharmaceuticals, access to the central nervous system via nose-to-brain delivery, and the potential to administer vaccines [1,2,3–10,11]. At the moment, spray pumps are the most commonly used devices for administering nasal products [12,13]. Even so, a significant amount of the product is deposited on the anterior vestibule, which is considered a less attractive region of the nasal cavity, probably due to inertial impaction of particles with Dv50 greater than 50 μm emitted with a relatively high velocity [12–14].

In addition to the delivery device and the characteristics of the drug formulation, the deposition site and the patient's use of the device can contribute to the efficacy of the formulation [15]. Although the characterization of nasal products is a critical point, there are still no recommendations or guidelines in terms of standard approaches for the evaluation of nasal deposition and/or dissolution profile of the formulation [16,17].

Several deposition studies have seen the use of transparent silicone nasal cavity models. Although Koken® nasal cast model primarily has an educational purpose, it can be used as a simple tool to visualise the deposition area of both powder and liquid formulations [18]. Another silicone nasal cavity replica was recently proposed by Optinose® [19]. In these deposition experiments, water finding colour-changing gels or pastes were used to highlight the regions where the liquid formulation was deposited. Kundoor and colleagues validated the use of Sar-Gel® (Sartomer Europe, Colombes, France) and studied the deposition of three different commercial products with and without vacuum pump aspiration [12].

The water finding Kolor-Kut® (Kolor Kut Products Co. ltd., Houston, TX, USA) was used successfully by Lungare and colleagues to execute a deposition study on the Koken nasal cast [20]. However, using these gels and pastes presents issues related to sensitivity and background interference. Hence, we introduced the use of fluorescence to visualize and quantify the deposition of a nasal liquid formulation in a transparent model of a nasal cavity. In this study, we were able to show excellent deposition characteristics, comparable with existing less patient-friendly nebulisers [21]. We did so using an innovative and simple spray pump emitting a spray with narrow droplet size distribution and volume median particle size (Dv50) between 15 and 25 μm at a low spray velocity.

Materials and methods

Calcein ($C_{30}H_{26}N_2O_{13}$) (Carl Roth, Karlsruhe, Germany) MW 622.55 g/mol was used as a fluorescent dye. The formulation of calcein (1 mg/ml) for the tests was prepared with a viscosity between 2 and 10 cP. The powder of calcein was solubilised in 80 μL of 1 M NaOH, to which 25 % (w/v) or 60 % (w/v) glycerol aqueous solution was added to obtain the respective viscosity of 2 and 10 cP and preserve fluorescence over time (Figure S1).

Nasal spray pumps attached to a 10 mL HDPE vial for the study are based on the 3 K® system from Aero Pump (Hochheim, Germany). They contain a standard swirl nozzle emitting 100 μL per actuation, or the optimized soft mist nozzle from Medspray (Enschede, the Netherlands) emitting 45 μL (Figure S2). The soft mist nozzle configuration contains 48 pores of 4 μm in diameter with a spray cone angle of 20°.

The study of the deposition pattern was carried out in both the presence and absence of a simulated inhalation flow, for which a Copley LCP5 vacuum pump (Copley Scientific, Nottingham, United Kingdom) was used. The airflow was controlled with a TSI 4040 flowmeter (TSI Inc., Shoreview, MN, USA). A silicone nasal cavity model produced by Koken® (Model LM-005 Koken ltd., Tokyo, Japan; Figure S3) was used to visualise the deposition area.

During the deposition experiments, the transparent septum was assembled to half of the cast in use. The spray pump device was manually actuated once and twice inside the nostril at a 45° angle in relation to the palate, and inserted 10 mm into the nostril. Before spraying, a first reference image was acquired using a white LED light. To detect the fluorescent dye, UV light CAMAG® UV Lamp (Muttenz, Switzerland) with a wavelength of 366 nm was used as a source of UV rays, and the camera was set with an exposure time of 1/15 s. The ratio of focal length to effective aperture diameter (f) was 5.6, with a focal distance of 16 mm and ISO 2000.

A black background was used and the positions and distances between the camera and the cast were fixated. The digital camera (Sony α 5100, Sony, Tokyo, Japan; 24.3 megapixels APS-C sensor) was placed 15 cm from the cast. The camera's optical lens was equipped with a yellow filter (vhbw©, Bischofswerda, Germany) to reduce background lighting of the lamp. Before each image acquisition, the septum was removed.

The extent of the deposition area and the deposition regions has been determined using the software ImageJ (U.S. National Institute of Health, Bethesda, MD, USA). The procedure was repeated three times for both the left and right sides of the cast. The image before spraying was converted to an 8-bit grayscale image, while the image acquired after spraying was converted to an 8-bit colour image (Figure S4). A graduated scale positioned near the cast allowed for the conversion of the number of pixels to mm². The left and right portion of the total cast's surface area were divided into arbitrarily constant regions of interest (ROIs) for all analysed images (Fig. 1).

The threshold level range was fixated between a minimum value of 11 and a maximum value of 256 for all images acquired after spraying. The coating extension was calculated on the whole portion of the cast, and within each individual ROI.

The quantitative analysis of the spray deposition by fluorometry was assessed and divided into two theoretical portions: the upper and the lower portion (Figure S5).

The fluorescent solution of calcein was sprayed twice consecutively, into the cast. The sample relating to the lower portion of the cast was obtained by inserting the cast inside a plastic container
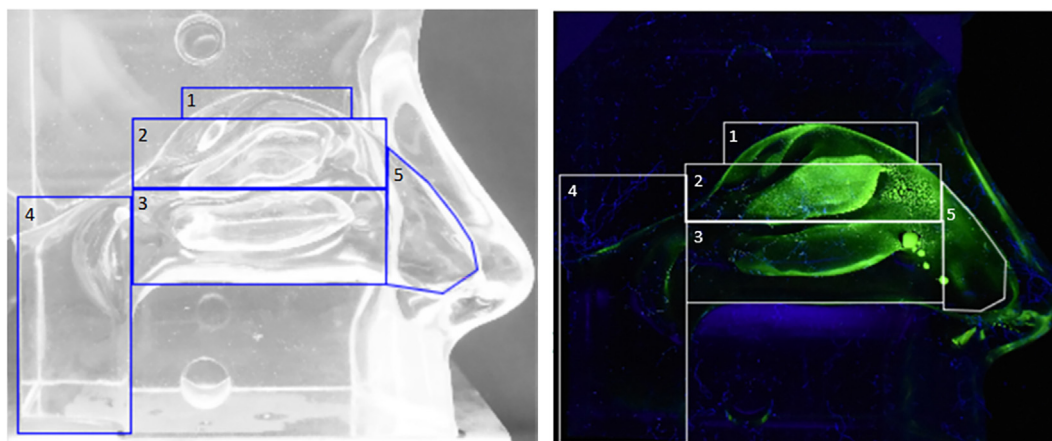
Fig. 1. Regions of Interest (ROI) obtained with the software ImageJ. 1: Olfactory region; 2: Middle turbinate; 3: Inferior turbinate; 4: Nasopharynx; 5: Vestibule.

measuring 5 × 12 × 7.5 cm, in which the cast was immersed in 220 mL of ultrapure water for 1 min and then removed carefully, avoiding splashes and ripples. The cast was then washed with 100 mL of ultrapure water to collect the fluorescence deposited on the upper portion of the cast. The calcein concentration in samples was determined using a Spark multimode microplate reader (TECAN, Mannendorf, Switzerland). The value of excitation was 495 and the emission was 535 nm. Ultrapure water was used in the formulation and collecting solvent was used as blank. The method was specific and linearity between 0.03 and 0.1 μg/ml was assessed.

The particle size distribution of the sprays was obtained using a Mastersizer S (Malvern Panalytical, Malvern, United Kingdom). The open bench configuration was employed, the devices were positioned 10 cm from the laser beam and 5 cm from the lens, and activated manually. The analysis was then elaborated according to MIE theory (refractive index 1.33; 3QAA) using the instrument software (ver. 2.19, Malvern Instruments ltd., Malvern, UK).

A Phantom Miro M310 high-speed camera (Vision Research ltd., Wayne, NJ, USA) at a frame rate of 1000 fps was used to record the spray plume dynamics. The droplets were illuminated against a dark background, using a bright light source under a slight angle with the camera's optical axis.

Results and discussion

High viscosity spray deposition pattern analysis

The deposition of the soft mist produced by Medspray's device, containing the high viscosity (10 cP) calcein aqueous solution, was analysed by selecting the range of (threshold) intensity levels between 11 and 256 (Figure S4).

The viscosity of 10 cP combined with the actuation angle of the device allowed for a deposition mainly in the upper portion of the cast, with a major impact on the middle turbinate. Interestingly, the deposition in the olfactory region of the nasal cavity corresponded to 8.45 % in the left section and 10.03 % in the right section. This was already the case after the first actuation, and around 7 % for both left and right sides after the second actuation (Table 1). Despite the encouraging results at a viscosity of 10 cP, a lower viscosity could improve the coverage of the formulation cast through control of droplet size distribution and velocity.

Quantitative analysis of the nasal cast deposition by fluorimetry

The fluorometric analysis could overcome the potential underestimation of the deposition in some areas of the cast, which are not completely visible from the projection of the cast.

Although the Koken® nasal cast cannot be physically divided into several parts to be analysed separately like other nasal casts [22], this simple subdivision obtained by differential immersion in a washing container made it possible to validate and support the data obtained by imaging. Most of the fluorescence (80 %) was found in the upper portion of the cast (see Figure S6). Analysis of the deposition images after the two actuations showed a greater amount of deposition in the upper part (sum of the ROIs of the middle turbinate and olfactory region). As expected, an underestimation of the deposition was demonstrated using the image analysis approach which was only 64.9 % (left side) and 55.6 % (right side).

Low viscosity spray deposition pattern analysis

A better distribution of the formulation on the cast was observed after reducing the viscosity of the formulation to a value of 2 cP. The deposition experiments were conducted under various experimental conditions, as shown in Table 2 (see Figures S7 and S8 as well). Although the droplets are distributed over a larger area without the inhalation flow, 19.5 % of the coating was found in the olfactory region when an inhalation flow of 30 LPM passed through a single nostril.

In Fig. 2A a standard swirl nozzle delivered 100 μL of calcein fluorescent solution, while in Fig. 2B the soft mist nozzle delivered 90 μL. The latter device produced a 30 % larger and more uniform coating extension than that obtained with a standard nasal pump spray device (see also Figure S8). This effect was also observed in a device with a soft mist nozzle with pores of 7 μm (Figure S7), likely related to the larger droplet size and aerosol velocity.

Intranasal droplet size deposition pattern analysis

We used the Medspray soft mist nozzle as the droplet source, which has an average initial droplet velocity of 0.8 m/s, in combination with a mild airflow of 10 L/min per nostril (Fig. 3).

Fig. 3B–D illustrates that droplets deposited in the turbinate regions are typically much larger (40–160 μm) than droplets deposited deeper in the turbinate region (10–40 μm) (Fig. 3B). This is caused by the fact that smaller droplets experience more air drag, making them more susceptible to the turbulent curved airflow in the turbinate region. The droplet velocity is also a critical parameter to control deposition in the nasal cavity.

Only droplets between 10 and 40 μm were found in the olfactory region (Fig. 3B). These droplets are emitted to a small extent from the standard swirl nozzle as demonstrated by the particle size distribution analysis (Figures S9 and S10). The ratio of the

Table 1
Extension of the deposition area for each analysed region.

| | Number of Device Actuations | | | |
| | 1 | 2 | 1 | 2 |
	Left Section (mm²)		Right Section (mm²)	
Inferior Turbinate	6.82 ± 4.98	9.11 ± 4.49	8.22 ± 5.71	9.23 ± 5.65
Middle Turbinate	72.94 ± 7.48	108.03 ± 22.10	59.21 ± 5.37	90.91 ± 5.01
Olfactory Region	9.42 ± 4.89	13.43 ± 7.09	10.60 ± 4.78	13.10 ± 8.40
Vestibule	21.00 ± 8.40	56.20 ± 15.20	29.48 ± 6.35	73.12 ± 8.62
Nasopharynx	0.03 ± 0.03	0.18 ± 0.03	0.34 ± 0.19	0.62 ± 0.17
Total	110.21 ± 5.11	186.95 ± 14.28	107.85 ± 11.85	186.98 ± 12.23

Table 2
Comparison of the extension of the area in the regions of the nasal cavity, with different devices and with or without inhalation flow.

Deposition Experiment Conditions					
Device	Soft Mist Nozzle (4 µm nozzle)	Soft Mist Nozzle (4 µm nozzle)	Soft Mist Nozzle (4 µm nozzle)	Standard Nozzle	Standard Nozzle
Inhalation Airflow (L/min)	0	15[*]	30[**]	0	0
Number of Actuations	2	2	2	1	2
Volume Delivered (µl)	45	45	45	100	30
Nasal Cast ROIs	Deposition Area (mm²)				
Inferior Turbinate	322.61	98.11	73.73	54.02	12.43
Middle Turbinate	461.36	240.90	338.44	158.27	126.34
Olfactory Region	186.00	61.15	109.76	83.72	20.85
Vestibule	104.66	67.18	37.01	30.80	42.74
Nasopharynx	9.26	0.84	3.21	3.56	0.17
Total	1083.60	468.19	562.16	330.37	202.55

[*] Airflow of 30 L/min through two nostrils.
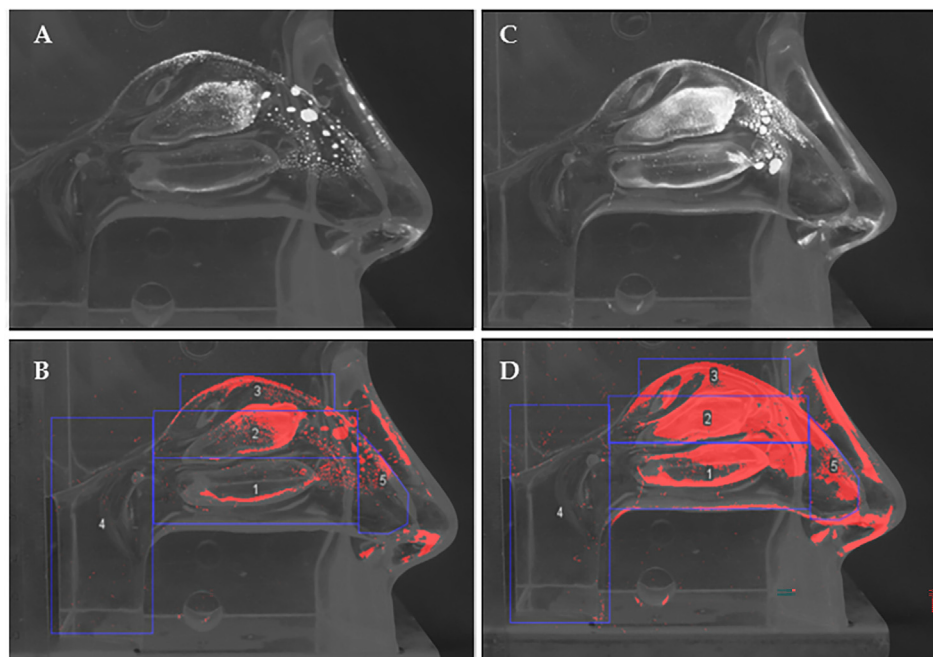[**] One nostril blocked.

Fig. 2. Coverage comparison: (A) Standard swirl nozzle spray deposition; (B) Selection of the deposition areas of A included in the threshold range; (C) Medspray soft mist nozzle spray deposition; (D) Selection of the deposition areas of C included in the threshold range.

centrifugal force for the Stokes air friction force of the droplets, scales linearly with the velocity of the droplets and scales square with the size of the droplets. In order to reduce this ratio, it is necessary to reduce both initial droplet velocity (ejection velocity) and droplet size.

Droplet velocity, droplet size and plume formation

To explain the large difference in droplet deposition for the soft mist nozzle and the standard swirl nozzle, we used high-speed photography to determine the initial droplet velocity and plume
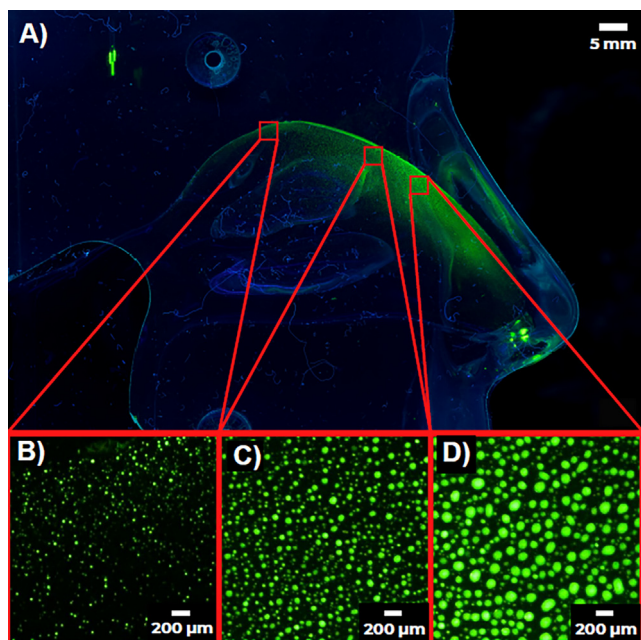
Fig. 3. Droplet size deposition pattern of a Medspray soft mist nozzle (at 10 L/min airflow): (A) Overview of the nasal cast deposition for one actuation; (B)–(D) Enlargements at different locations in the upper turbinate region. There is a clear decrease in the average drop size further down the intranasal region.

Fig. 4. Droplet trajectories for the two spray nozzles (A) The Medspray soft mist nozzle; (B) Magnification of the marked area in (A) can be observed as indicated by the arrows. (C) The standard swirl nozzle. (D) Magnification of the marked area in (C), Straight droplet trajectories can be observed as indicated by the arrows. See corresponding videos for the plume dynamics.

formation (Figure S11). The spray of the swirl nozzle has an initial velocity of about 13 m/s, spraying a total volume of 100 μL in approximately 100 ms. However, the spray of the Medspray nozzle has a much lower initial velocity of about 0.7 m/s, and sprays 45 μL in 500 ms (videos available as Supplementary Materials). Furthermore, the Medspray soft mist nozzle produces much smaller droplets (Dv50 15–25 μm) than the standard swirl nozzle (Dv50 60 μm) (Figures S9 and S10).

The standard swirl nozzle produces a short burst of droplets, all travelling upwards in straight trajectories (Fig. 4C and 4D). In contrast, the Medspray mist nozzle produces droplets in a turbulent droplet cloud (Fig. 4A and 4B).

The ballistic trajectories of the swirl nozzle droplets indicate that most droplets are deposited only at the start of the nasal cavity. In fact, the medium droplet size is determined by a competition between the surface tension of the liquid and inertia [23]. In this case the medium drop size scale is $v^{-2/3}$, v being the velocity. In practice, this means that small enough droplets for nasal administration can only be obtained by increasing the velocity. The droplet size of the Medspray soft mist nozzles is mostly determined by the hole diameter and is therefore independent of the spray velocity. This explains why the Medspray soft mist nozzle leads to better coverage, as both droplet size and droplet velocity are smaller.

Conclusions

In this work, a method for quantifying silicone nasal cast deposition of liquid formulations using nasal devices was optimised. A formulation containing a fluorescent molecule made it possible to accurately determine the amount of coverage on the nasal cast in different regions using images analysis. Image quantification was completed by fluorometric analysis. The used method allowed for the comparison of the deposition area and regions reached by the formulation emitted by nasal devices. We found that droplet velocity is a critical parameter in the deposition in the nasal cavity. Using standard swirl nozzles, many droplets are found on the
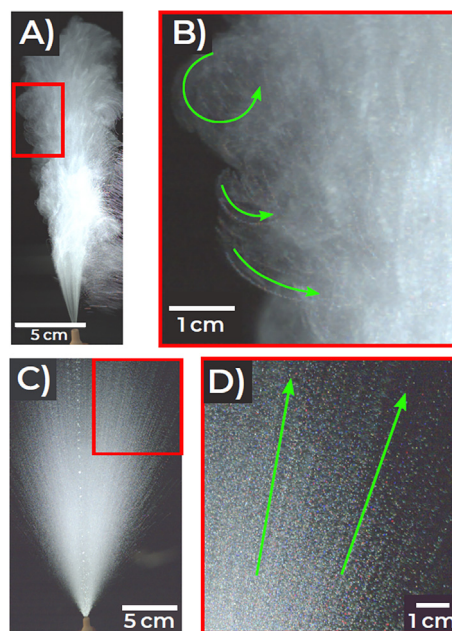
surface of the nasal vestibule due to deposition and accumulation of large primary droplets with a large initial velocity (>10 m/s) of the liquid sprayed. Medspray soft mist nozzles produce smaller droplets at a much lower initial velocity (<1 m/s), resulting in a more uniform coverage.

Compliance with ethical standards

The authors have disclosed potential Conflic of Interest in a separate document.

The present study does not involve animals or human subjects.

*In any case, the authors declare that the present research has been conducted and presented in this manuscript in accordance to Publishing Ethics adopted by Elsevier (*https://www.elsevier.com/about/policies/publishing-ethics#Authors*)*

CRediT authorship contribution statement

Davide D'Angelo: Investigation, Methodology, Formal analysis, Writing - original draft. **Stefan Kooij:** Investigation, Methodology, Formal analysis, Writing - original draft. **Frank Verhoeven:** Funding acquisition, Resources. **Fabio Sonvico:** Supervision, Conceptualization, Writing - review & editing. **Cees van Rijn:** Supervision, Conceptualization, Writing - review & editing.

Declaration of Competing Interest

The authors declare that they have no known competing financial interests or personal relationships that could have appeared to influence the work reported in this paper.

Acknowledgements

Appendix A. Supplementary data

Supplementary data to this article can be found online at https://doi.org/10.1016/j.jare.2022.04.011.

References

[1] Sacchetti C, Artusi M, Santi P, Colombo P. Caffeine microparticles for nasal administration obtained by spray drying. Int J Pharm 2002;242:335–9. doi: https://doi.org/10.1016/S0378-5173(02)00177-1.

[2] Russo P, Sacchetti C, Pasquali I, Bettini R, Massimo G, Colombo P, et al. Primary microparticles and agglomerates of morphine for nasal insufflation. J Pharm Sci 2006;95(12):2553–61.

[3] Torres LM, Trinidad JM, Calderón E, Benitez D, Perelman M. Fentanyl pectin nasal spray for breakthrough cancer pain. Int J Palliat Nurs 2015;21:114–6. doi: https://doi.org/10.12968/ijpn.2015.21.3.114.

[4] Targum SD, Daly E, Fedgchin M, Cooper K, Singh JB. Comparability of blinded remote and site-based assessments of response to adjunctive esketamine or placebo nasal spray in patients with treatment resistant depression. J Psychiatr Res 2019;111:68–73. doi: https://doi.org/10.1016/j.jpsychires.2019.01.017.

[5] Cady R. A novel intranasal breath-powered delivery system for sumatriptan: A review of technology and clinical application of the investigational product AVP-825 in the treatment of migraine. Expert Opin Drug Deliv 2015;12:1565–77. doi: https://doi.org/10.1517/17425247.2015.1060959.

[6] Pires A, Fortuna A, Alves G, Falcão A. Intranasal drug delivery: how, why and what for? J Pharm Pharm Sci 2009;12:288–311. doi: https://doi.org/10.18433/j3nc79.

[7] Craft S, Claxton A, Baker LD, Hanson AJ, Cholerton B, Trittschuh EH, et al. Effects of regular and long-acting insulin on cognition and Alzheimer's disease biomarkers: a pilot clinical trial. J Alzheimer's Dis 2017;57(4):1325–34.

[8] Quintana DS, Westlye LT, Hope S, Nærland T, Elvsåshagen T, Dørum E, et al. Dose-dependent social-cognitive effects of intranasal oxytocin delivered with novel Breath Powered device in adults with autism spectrum disorder: a randomized placebo-controlled double-blind crossover trial. Transl Psychiatry 2017;7(5):e1136.

[9] Cheng Y-H, Dyer AM, Jabbal-Gill I, Hinchcliffe M, Nankervis R, Smith A, et al. Intranasal delivery of recombinant human growth hormone (somatropin) in sheep using chitosan-based powder formulations. Eur J Pharm Sci 2005;26(1):9–15.

[10] Thorne RG, Pronk GJ, Padmanabhan V, Frey WH. Delivery of insulin-like growth factor-I to the rat brain and spinal cord along olfactory and trigeminal pathways following intranasal administration. Neuroscience 2004;127(2):481–96.

[11] Jahnsen FL, Gran E, Haye R, Brandtzaeg P. Human Nasal Mucosa Contains Antigen-Presenting Cells of Strikingly Different Functional Phenotypes. Am J Respir Cell Mol Biol 2004;30:31–7. doi: https://doi.org/10.1165/rcmb.2002-0230OC.

[12] Kundoor V, Dalby RN. Assessment of nasal spray deposition pattern in a silicone human nose model using a color-based method. Pharm Res 2010;27:30–6. doi: https://doi.org/10.1007/s11095-009-0002-4.

[13] Suman, D.Julie Laube, L. Beth Dalby R. Comparison of Nasal Deposition and Clearance of Aerosol Generated by a Nebulizer and an Aqueous Spray Pump 1999:1648–52.

[14] St. Martin MB, Hitzman CJ, Wiedmann TS, Rimell FL. Deposition of aerosolized particles in the maxillary sinuses before and after endoscopic sinus surgery. Am J Rhinol 2007;21(2):196–7.

[15] Merkus P, Ebbens FA, Muller B, Fokkens WJ. Influence of anatomy and head position on intranasal drug deposition. Eur Arch Oto-Rhino-Laryngology 2006;263:827–32. doi: https://doi.org/10.1007/s00405-006-0071-5.

[16] Salade L, Wauthoz N, Goole J, Amighi K. How to characterize a nasal product. The state of the art of in vitro and ex vivo specific methods. Int J Pharm 2019;561:47–65. doi: https://doi.org/10.1016/j.ijpharm.2019.02.026.

[17] Forbes B, Bommer R, Goole J, Hellfritzsch M, De Kruijf W, Lambert P, et al. A consensus research agenda for optimising nasal drug delivery. Expert Opin Drug Deliv 2020;17(2):127–32.

[18] Buttini F, Colombo P, Rossi A, Sonvico F, Colombo G. Particles and powders : Tools of innovation for non-invasive drug administration. J Control Release 2012;161:693–702. doi: https://doi.org/10.1016/j.jconrel.2012.02.028.

[19] Djupesland PG, Messina JC, Mahmoud RA. Role of nasal casts for in vitro evaluation of nasal drug delivery and quantitative evaluation of various nasal casts. Ther Deliv 2020;11:485–95. doi: https://doi.org/10.4155/tde-2020-0054.

[20] Lungare S, Bowen J, Badhan R. Development and evaluation of a novel intranasal spray for the delivery of amantadine. J Pharm Sci 2016;105:1209–20. doi: https://doi.org/10.1016/j.xphs.2015.12.016.

[21] Vecellio L, De Gersem R, Le Guellec S, Reychler G, Pitance L, Le Pennec D, et al. Deposition of aerosols delivered by nasal route with jet and mesh nebulizers. Int J Pharm 2011;407(1-2):87–94.

[22] Azimi M, Longest PW, Hindle M. Towards clinically relevant in vitro testing of locally acting nasal spray suspension products. Respir Drug Deliv Eur 2015;121–30.

[23] Kooij S, Sijs R, Denn MM, Villermaux E, Bonn D. What determines the drop size in sprays? Phys Rev X 2018;8:31019. doi: https://doi.org/10.1103/PhysRevX.8.031019.